Robotic automation of "blind" and two-photon targeted patch-clamp electrophysiology *in vivo*

Gema I Vera Gonzalez*, Phatsimo O Kgwarae*, Luca A Annecchino, and Simon R Schultz

Centre for Neurotechnology and Department of Bioengineering,
Imperial College London, London SW7 2AZ, UK

1 Introduction

Patch-clamp electrophysiology is among the most reliable methods for monitoring single neuron function and determining cell type, despite the high dexterity required and relatively low throughput. The use of the patch-clamp technique in live animal preparations has traditionally been limited to "blind" (non-visually-targeted) recordings (Pei et al., 1994; Margrie et al., 2002). Robotic automation has improved throughput without compromising the quality and the duration of recordings (Kodandaramaiah et al., 2012; Annecchino and Schultz, 2018) and can encourage the diffusion of the technique. Combining automated patch-clamp with two-photon imaging allows selection of specific cell types and has the potential to integrate anatomical, physiological and pharmacological information, therefore reconciling target cell characteristics and network behaviour (Annecchino et al., 2017; Suk et al., 2017). Importantly, this affords the capability to test hypotheses concerning how circuits involving particular cells or cell types operate during physiological and pathological states.

The advantages of robotic patch-clamp can potentially be even more impactful when attempting simultaneous recordings from multiple cells (Markram et al., 1997; Crochet and Petersen, 2006; Kodandaramaiah et al., 2018). Paired patch-clamp recordings enable unambiguous measurements of the connectivity between two neurons and allow testing for the presence of both electrical and chemical connections with high temporal accuracy, as well as revealing subthreshold correlations. These also have the potential to provide even more complex biological information in single-cell transcriptomics (Cadwell et al., 2016; Mun et al., 2020). For example, transcriptomic changes underlying neuronal computation and development can be effectively studied. Comparable sensitivity enabling the detection of synaptic connectivity has not yet been routinely demonstrated with other techniques such as genetically-encoded calcium indicators (GECIs) like GCaMP, or genetically-encoded voltage sensors (Lin and Schnitzer, 2016; Yang and St-Pierre, 2016). Given the technical difficulty of performing multiple *in vivo* patch-clamp recordings, robotic automation appears very promising. With increasing automation of other experimental steps - craniotomies (Ghanbari et al., 2019), trajectory obstacle avoidance (Stoy et al., 2017), pulsatile motion prediction and correction (Stoy et al., 2021) and pipette reuse (Kolb et al., 2016; Landry et al., 2021) - there is the potential for further reduction in experimental variability due to human factors.

2 Overview of the technical specifications

2.1 Experimental setup

Automatic whole-cell recording systems have been implemented using standard hardware and software available in conventional *in vivo* electrophysiological setups (Annecchino and Schultz, 2018). This includes one or more micromanipulators, a signal amplifier, a digital/analogue acquisition board, a data acquisition software and a personal computer. The only unconventional components are (1) an electropneumatic pressure regulator system to control the internal pressure of the pipette, and (2) an algorithm to monitor the pipette impedance signal in real time, and execute pressure and manipulator controls accordingly. Such a system is sufficient for performing automated "blind" whole cell recording (WCR).

Two-photon guided WCR requires a two-photon microscope in addition to tissue labelled with fluorescent reporters (Fig. 1). This consists of a commercial mode-locked laser (such as a Ti:Sapphire laser) and two galvanometric scanning mirrors (or alternative sample scanning device such as acousto-optic deflectors). The resulting fluorescence signal is split into specific wavelength bands by dichroic beam splitters and optical filters, and collected by one or more photo-multiplier tubes (detectors). Two-photon images of fluorescently labelled cells are reconstructed and streamed, in real-time, to dedicated software responsible for object identification, target selection and tracking. Tracking information is then used to control the manipulator and adjust the trajectory and dynamics of pipette navigation towards the target.

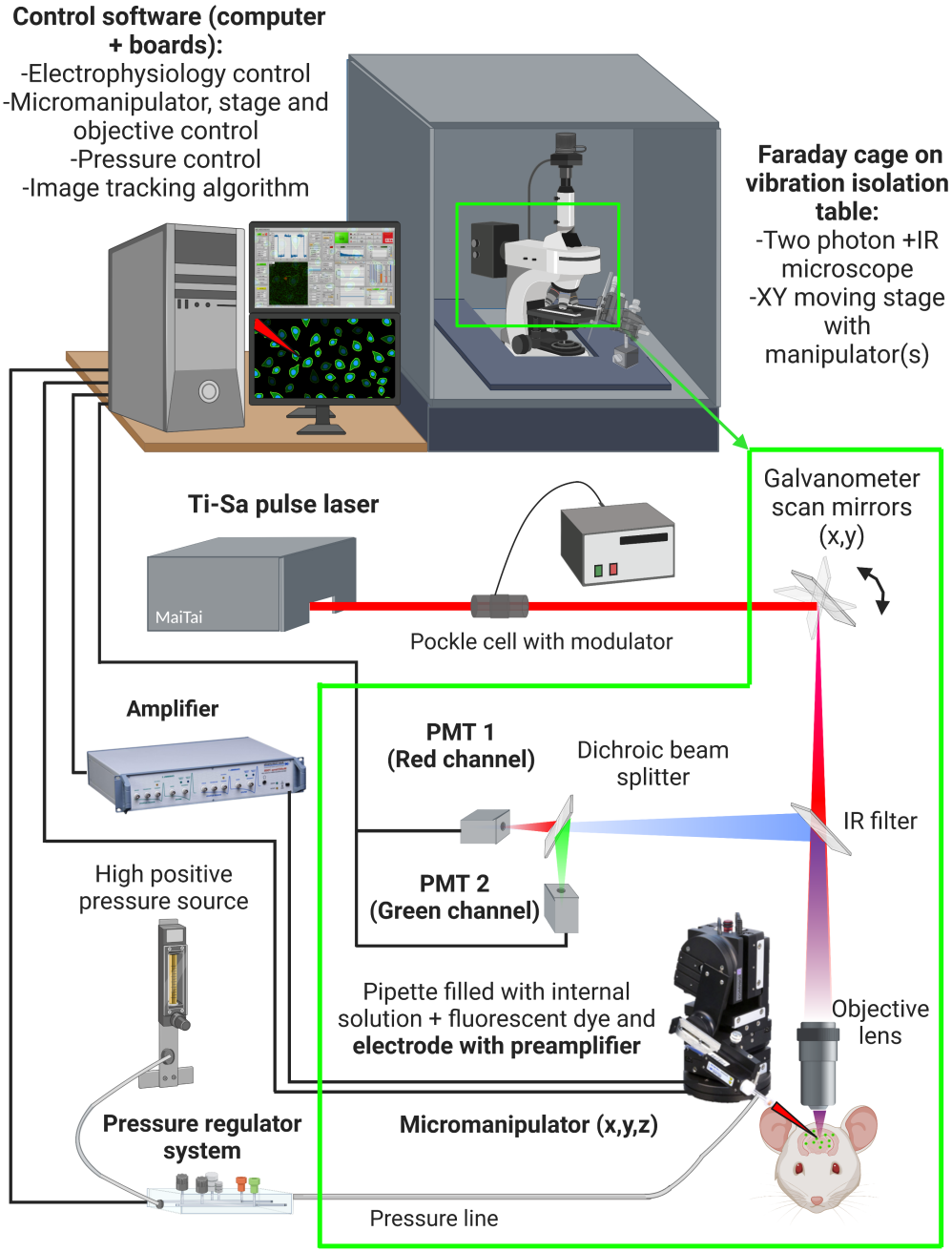

Fig. 1. Two-photon guided patch-clamp setup. It consists of a conventional commercial two-photon microscope, a mode-locked Ti-Sapphire laser, a patch setup equipped with a programmable three-axis micromanipulator, a signal amplifier, an analogue to digital converter board, a computer, and a custom-made electro-pneumatic actuator for controlling micropipette internal pressure. "Blind" patch-clamp is achieved with the same setup but excluding the imaging components (microscope and laser). Adapted from Annecchino et al. (2017).

Finally, in both "blind" and image-guided experiments, sealing and break-in are performed automatically by the computer-controlled pressure system.

2.2 Pipette navigation and target cell engagement

The insertion of a sharp electrode into soft tissue leads to non-negligible mechanical strain and stress. The mechanical response of the tissue undergoing morphological deformation may change the shape and position of the target. Therefore we need to compensate for pipette-induced movements while moving

the pipette through the tissue. One way to do this is by persistently monitoring the target position using a computer vision tracking algorithm, and using it to provide closed-loop visual servoing for controlling pipette navigation. Automatic fine control of the pipette position for navigation and target engagement relies on real-time analysis of the light signature of the fluorescent targets in the tissue. During the target engagement procedure, the position of the target is continuously reassessed and the approach trajectory of the pipette re-adjusted.

2.3 Automated analysis of two photon images and visual feedback

Automated two-photon targeted patch-clamp systems developed so far have used similar image analysis methods, with some small differences such as programming language and image processing libraries used. OpenCV is an example of such a library, and is compatible with multiple platforms including Python, C, C++ and Java. It is used in the system by Wu et al. (2016)(Python). MATLAB (Mathworks, Natick, MA, USA) has a dedicated Image Processing toolbox and has been used by Long et al. (2015) and Suk et al. (2017), while similar capabilities are offered by the IMAQ suite available for LabVIEW (National Instruments, Austin, TX, USA), used by Annecchino et al. (2017).

Commercial two-photon microscope acquisition software (e.g. LabView-based SciScan, Scientifica Ltd, or MATLAB-based ScanImage, Vidrio Technologies LLC) can be used to acquire and stream image frames to an automated image analysis modules in the system. Image averaging, optimisation and segmentation ((Otsu, 1979)), are then used to detect salient objects in the scene, separate bright cell(s)/pipette(s) from the background and identify candidate targets. The system described by Annecchino et al. (2017) performs local thresholding: a spatial modulation of the threshold value by dividing the image into windowed segments and then calculating a threshold value specific to that local neighbourhood of pixels. Global thresholding can be a viable approach if it accounts for inter-object intensity variation. Such an algorithm might involve performing multiple segmentations over a range of threshold values followed by a selection of the threshold value that gives the closest match for the target segment to a stored reference, similar to methods used by (Wu et al., 2016; Suk et al., 2017). All salient objects are then geometrically classified in terms of area, contour, bounding rectangle and centre of mass and used to define a set of pixel masks. Measurements from pixel intensities within the masks can then be used to assess the depth and degree of focus of the neuron target(s).

Focus and depth can be assessed by measuring the sharpness of the identified object contour. This can be calculated as the difference between the average intensity of the pixels belonging to the internal boundary region of the object and the average intensity of the pixels belonging to the external boundary region, normalised by the average intensity of pixels within the internal boundary region (Annecchino et al., 2017). The target's depth is taken as the z-position of the focal plane of maximum contrast or intensity. If "shadowpatching"- using an extracellular dye to produce 'shadows' of the cells (they would appear as the negative parts of the image) (Kitamura et al., 2008), a different approach should be adopted for target tracking. In this context, the reduced axial variation in the fluorescence signal one would have with individually labelled neurons, makes it more challenging to determine a target's z-coordinate. An alternative approach could be based on morphological feature matching to establish and follow a target's position.

2.4 Expanding to automated *in vivo* multipatching

Robotic patch-clamp has been scaled up to allow the independent control of up to four micropipettes and obtain blind WCRs from up to three different neurons at the same time in the neocortex of both anaesthetised and awake animals (Kodandaramaiah et al., 2018). This system obtained a dual or a triple WCR in 18% of the trials in awake mice and 29% of trials on anaesthetised mice. The relative decrease in performance when attempting multiple recordings is related to the fact that each electrode moves and encounters a cell at different times. This aspect, compounded with the different gradients of tissue deformation induced by each electrode, can be challenging especially when it is critical to prevent any relative motion between the pipette tip and the target cell (i.e., during sealing). Additionally, in a blind paradigm there might the possibility of pipette collision. Visual targeting, can likely prevent pipette collision and potentially enable strategies to compensate for tissue and target deformation induced by multiple penetrating electrodes, but it does not eliminate them completely. Additionally, concurrent navigation control of multiple electrodes and the tracking of their target cells can be a comparatively demanding task due to the limited depth-of-field of two-photon imaging. Generally, an all-at-once strategy whereby sealing is attempted at the same time after all electrodes are in close contact with their target

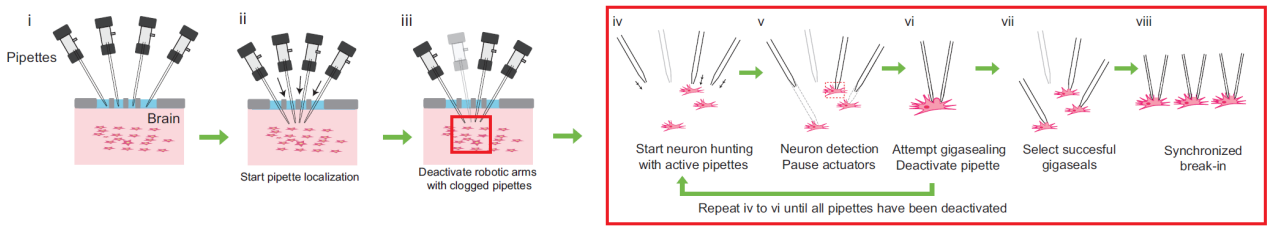

Fig. 2. Steps of the multipatcher algorithm (Kodandaramaiah et al., 2018). (i) Manual positioning of the pipette tips on the brain surface. (ii) Automatic positioning of the tips over the target brain region and initiation of neuron hunting. (iii) Deactivation of clogged pipettes. (iv) Simultaneous movement of the tips in small steps until (v) a cell is detected. (vi) Sealing is initiated while all other pipettes remain motionless. (vii) Steps (iv)-(vi) are repeated until all pipettes have attempted a seal. (viii) Break in is attempted in seals with resistance above 1 GΩ, simultaneously. Adapted from Kodandaramaiah et al. (2018).

cell, appears to be relatively more successful than one-at-a-time strategy (Kodandaramaiah et al., 2018). The steps of the multipatcher algorithm by Kodandaramaiah et al. (2018) are depicted in Fig. 2.

2.5 Control of pipette internal pressure

The precise and timely control of the pipette internal pressure is crucial for i) keeping the pipette tip clean, ii) obtaining a good seal, and iii) effectively rupturing the patch membrane and achieving a stable whole cell recording configuration to yield high quality recording. Traditionally, the pipette internal pressure is controlled manually by means of a three-way valve and a syringe, and the experimenter uses their mouth to apply suction to help form the seal and break into the cell (Hamill et al., 1981; Margrie et al., 2002; DeWeese, 2007).Several custom-built electro-pneumatic control devices have been implemented as part of robotic "blind" and image guided patch-clamp systems (Kodandaramaiah et al., 2012; Perin and Markram, 2013; Wu et al., 2016; Annecchino et al., 2017; Suk et al., 2017; Holst et al., 2019; Peng et al., 2019; Kolb et al., 2019; Koos et al., 2021) but they can be potentially used as part of classic manual patch-clamp setups to minimise human error and increase precision and sensitivity. Those systems typically employ solenoid valves, one or more pressure sensors, a positive pressure source (air pump, compressed air tank or outlet) and either a negative pressure source or a vacuum ejector (Fig. 3). All the components can be connected by silicone or polyurethane tubes or alternatively attached to a plastic platform with drilled in reservoirs (Annecchino et al., 2017). The airflow through each valve in the system can be controlled with some basic electronics components and data acquisition/control board (i.e., National Instrument DAQ Boards) or a dedicated micro-controller (i.e., Arduino board) running a

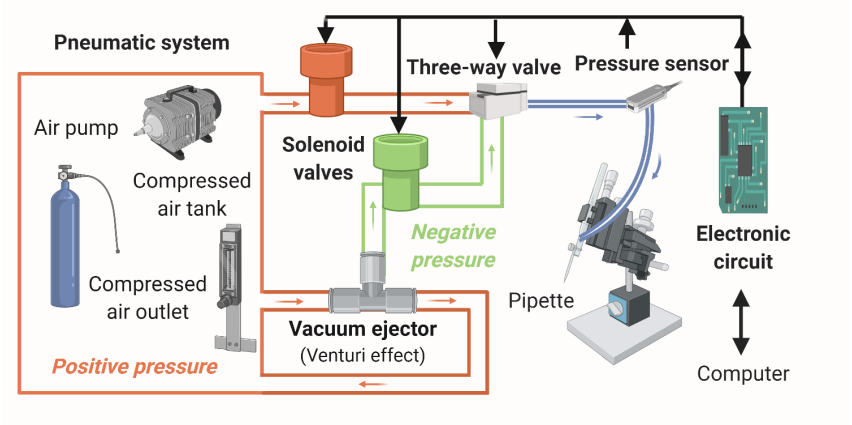

Fig. 3. Pressure system. Solenoid valves modulate the airflow in the system and are controlled in closed-loop by an electronic circuit and maintain a stable pressure output. Negative pressure (suction) can be generated by a vacuum ejector or alternatively sourced from another pump or reservoir. A 3-port valve selects either the positive or the negative pressure branch to the output to manipulate the pipette internal pressure. The sensor is positioned as close as possible to the output. A microcontroller reads the pressure signal(s) from the sensor(s) and regulates all the valves as required.

proportional-integrative-derivative (PID) algorithm for closed-loop control (see Annecchino et al. (2017)). An automatic pressure control system is also necessary to automatise a pipette cleaning process and afford the possibility of reusing the same pipette for multiple patching attempts by cleaning them in between trials (Kolb et al., 2016).

These electro-pneumatic systems can be assembled relatively easily, with instructions available in Desai et al. (2015); Kodandaramaiah et al. (2016); Wu and Chubykin (2017), or bought commercially (Sensapex, Neuromatic devices).

3 Practical Tips

The patch electrodes and capillaries typically used for automated patch-clamp are the same as those used in manual methods. For two-photon guided experiments, the internal solution is augmented with a fluorescent dye (e.g. 50 μM Alexa Fluor 594) to make the pipette visible under laser excitation.

However, dye filled pipettes can release large amounts of fluorescent internal solution and create substantial background fluorescence which will eventually degrade image contrast and the ability to visualise the pipette and target cells. One alternative to fluorescent dyes is coating the pipettes with quantum-dots to make them visible under two-photon imaging while avoiding diffusing fluorescent internal solution and degrading contrast. Quantum-dot-coated pipettes seems to be visible even at larger depths when compared to dye filled ones and yield recordings of comparable quality to non-coated glass pipettes (Andrásfalvy et al., 2014).

Pipette tip coordinate updates rely on position readouts from the micromanipulator. These position values carry some level of uncertainty due to the limited precision of the micromanipulator. In addition, unwanted movements from drift and backlash may compound errors even further. These are unintended movements when the device is stationary and excess movements at the end of intended motions respectively. Therefore, when selecting micromanipulators, consideration should be given to devices with the highest precision, drift and backlash control. Also worthy of mention is the fact that old manipulators tend to become more imprecise and may drift, which is acceptable in manual patch but will lead to imprecise approaches in autopatchers.

4 Data Acquisition

4.1 Procedures for robotic "blind" and two-photon guided whole-cell recordings *in vivo*

Depending on the level of automation, the system can automatically perform all the steps involved in the patch-clamp experiment or only a subset (see section 5). In two-photon guided experiments, object identification and tracking information control manipulator movements that guide pipette navigation towards the target. In blind experiments, however, the algorithm makes decisions and executes timed actions solely based on the temporal trajectory of the pipette impedance. The simplified stages of an automated algorithm for both "blind" (B) and image guided (I) experiments are presented in Fig.4 and described as follows:

- **Setup (B/I):** The experimenter fills the pipette with internal solution (B) augmented with a fluorescent dye (I), then loads it into the pipette holder and automatically sets the internal pressure to a relatively high value (50-100 KPa). The pipette is manually placed at the centre of the field of view (I) or craniotomy (B) and is manually or automatically driven to the desired depth (i.e. brain surface).
- **Start imaging (I):** The low-magnification objective is exchanged for a water immersion one, and after forming an aCSF meniscus, image acquisition is initiated. The dye-filled pipette tip and fluorescently labelled cells are visualised using two-photon imaging. A computer vision algorithm identifies fluorescent objects within the streamed images.
- **Acquire pipette tip and target location (I):** The imaging system focuses on either the pipette(s) or the target(s), then these are automatically detected or selected manually and their location coordinates stored. The system automatically calculates the path of the pipette(s) to the target(s).
- **Cell hunting (B/I):** The pipette internal pressure is reduced to a lower positive value ($\sim$10 KPa). If the pipette is not blocked (determined by the impedance), the manipulator is moved in small steps ($\sim$2 μm) until a cell is encountered (B) or the targeted cell is reached (I). (I) The system continually monitors the target position and makes adjustments to the pipette trajectory to compensate for any

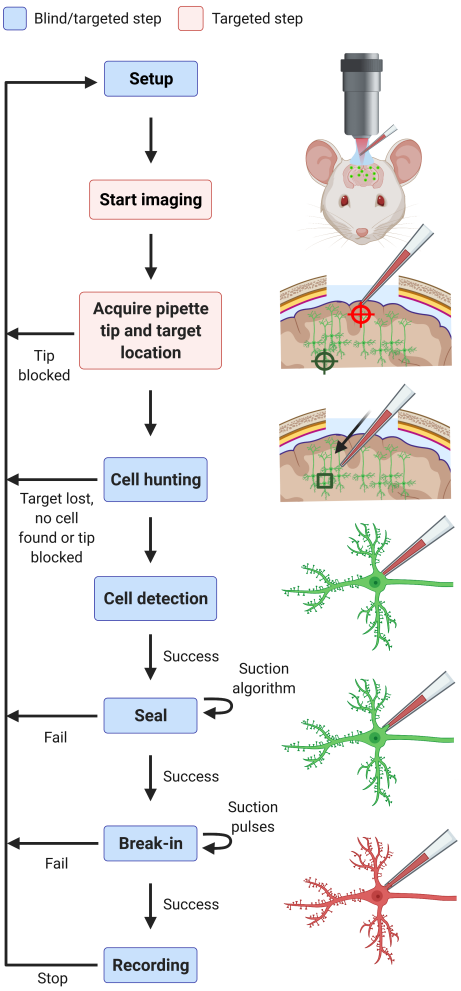

Fig. 4. Automated whole-cell patch-clamp procedure. (Left) Block diagram of the automated patch procedure. Steps in blue are common to both "blind" and targeted patch while additional steps for the two-photon guided patch are shown in light red. (Right) Schematic representation of the robotic patching procedure: Setup and pipette placement, tip and target coordinate acquisition, pipette positioning, automatic approach, target cell detection, seal formation, and break-in followed by whole-cell recording. Adapted from Annecchino et al. (2017).

tissue movement until the target is engaged. Note that while this step occurs in both blind and two-photon targeted mode, in the former case it is true "hunting", whereas in the latter, the presence of a cell in the locality is known, and the object is merely to precisely localise its position.

- **Cell detection (B/I):** A monotonic increase in impedance levels over two or more consecutive steps implies that a cell has been detected.
- **Seal (B/I):** At this point, the system automatically releases the internal pressure to allow the cell membrane to establish contact with the tip. To facilitate the seal, the pipette potential can be set to a negative value close to that of the intracellular potential of the cell ($\sim$ -65 mV). A light suction may be applied to form a tight seal. These can be executed through a set of control algorithms. A seal is obtained when the pipette resistance is constantly higher than a user defined seal threshold (usually 1-1.5 GΩ or 'gigaseal').
- **Break-in (B/I):** A WCR is achieved by breaking the patch membrane with one or more suction pulses. The automatic detection of a drop in the impedance signal and relative increase in current indicates a successful break-in.
- **Cell recording (B/I):** A successful break-in and viable WCR configuration is confirmed (i) electrophysiologically by verifying properties like membrane potential, firing properties, access resistance (B/I) and also (ii) optically observing the gradual filling of the target cell with fluorescent internal solution (I). At this point the recording can begin.

4.2 Example recordings from "blind" (single and multi-neuron) and targeted *in vivo* patch-clamp experiments

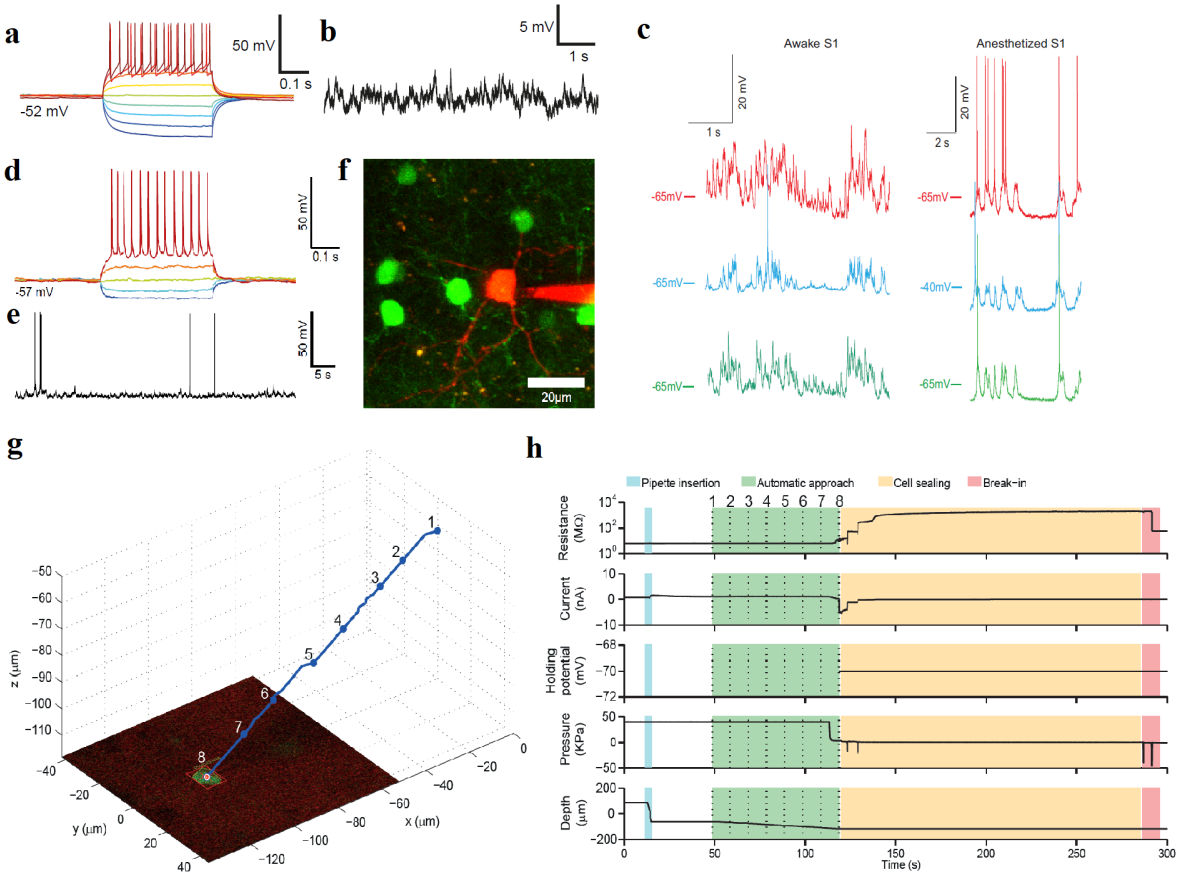

Fig. 5. (a,b) Example of an automatic "blind" whole cell single recording *in vivo*. (a) Intrinsic response of a neuron in the mouse cortex during hyperpolarising and depolarising current injections applied through the recording pipette electrode (400 ms-long pulses from -100 to +100 pA in 25 pA steps) and (b) recording for the same neuron at rest. Figures adapted from (Annecchino, 2016) (c) Examples of automatic blind whole cell multi recording *in vivo*. On the left, voltage recordings from three different neurons that were patched at the same time in S1 (somatosensory cortex) of an awake head-fixed mouse. On the right, same but for anaesthetised. Figures adapted from (Kodandaramaiah et al., 2018) (d,e) Example of a robotic two photon targeted whole cell single recording *in vivo*. Same as (a,b) but for a GAD67-GFP positive interneuron in the mouse cortex. Current injected in 400 ms-long pulses from -100 to +100 pA in 50 pA steps. Figures adapted from (Annecchino et al., 2017) (f) Two-photon image of the same neuron as (d,e). (g,h) Pipette approach trajectory and state during a typical robotic two photon targeted single patching process.(g) Automatic navigation of the pipette toward the target cell, with real-time feedback control of trajectory enabled.(h) Example of time-courses of pipette resistance, current, holding potential, internal pressure and pipette depth during the patching procedure (stages color coded; numeric labels correspond to points on the approach trajectory in (g). Time intervals relative to the different stages of the automated patching algorithm are colour coded. Figures adapted from (Annecchino et al., 2017)

5 Performance evaluation

Success rates for automated experiments *in vivo* have matched or exceeded manual approaches (Annecchino and Schultz, 2018). However, they are still dependent on high quality experimental preparation, and good internal solution composition.

Table 1 has a summary of the *in vivo* systems developed thus far. The autonomous degree represents the steps that have been automated within the patch-clamping pipeline according to the following: [1] Pulling pipettes [2] Filling the pipette with internal solution [3] Placement of the pipette on the electrode

holder [4] Pipette detection under microscope [5] Navigation of the pipette towards sample [6] Final cell approach [7] Pressure control [8] Sealing and break-through. However, it should be noted that these are not the only steps being automated, as the first strides towards the automation of craniotomies have been taken (Ghanbari et al., 2019; Rynes et al., 2020).

Paper and year	Anaesthetised or awake	Number of manipulators	Imaging system	Autonomous degree	WCR yield	Time (min)
Kodandaramaiah et al. (2012)	AN	1	"Blind"	[5][6][7][8]	32.9% in C57BL/6 mice	5 ± 2
Long et al. (2015)	AN	1	Two-photon targeted	[4][5][6]	(Manual) 66% in Cux2 mice and 22% in SST mice	6.55 ± 0.53
Desai et al. (2015)	AW	1	"Blind"	[4][5][6][7][8]	17.9% in C57BL/6 mice	5
Annecchino et al. (2017)	AN	1	Two-photon targeted	[5][6][7][8]	22.2% in GAD67-GFP mice	6.1 ± 0.6
Suk et al. (2017)	AN	1	Two-photon targeted	[4][5][6][7][8]	22.2% in PVCre x Ai14 mice, and 20% in CaMKIIa-Cre x Ai14 mice	10 ± 3
Kodandaramaiah et al. (2018)	AN and AW	4	"Blind"	[5][6][7][8]	30.7% (AN) and 17.5% (AW) of recordings were dual or triple recordings, 0% were quadruple, all in C57BL/6 mice.	10.5 ± 2.6 for one or more successful WCR
Holst et al. (2019)	AN	1	"Blind"	[2][3][4][5][6][7][8]	9% in C57BL/6 mice	5.3

The time column represents the minutes that the automated steps took, which is relevant not only for time-efficiency purposes but also for yield, as there is a negative correlation between time taken to break-in from pipette insertion and its success rate (Jouhanneau and Poulet, 2019). Yields should, however, be evaluated cautiously as each platform had slightly different conditions for considering a whole-cell recording successful and different techniques are expected to have different yields. For example, "blind" patching has higher yields than two-photon targeted patching (Jouhanneau and Poulet, 2019), as demonstrated by the fact that Annecchino et al. (2017) had 51.4% success rate when "blind"-patching, which is far above the reported 22.2% for targeted. Furthermore, one should also bear in mind that awake mice will always yield lower success rates than anaesthetised.

On the whole, for automated "blind" patch-clamp, around 75% of attempts lead to a seal and around 50% attempts lead to a WCR within 3-4 minutes on average (Annecchino et al., 2017). Dual or triple concurrent automated blind WCR have also been achieved around 29% of attempts in anesthetized

animals and 18% of attempts in awake animals within around 10 minutes on average (Kodandaramaiah et al., 2018).

Automated two-photon targeting achieved seals in about half of the trials and between 20-30% of those successful seals led to a WCR within a 6-minute average (Annecchino et al., 2017; Suk et al., 2017). Recordings were comparable in quality and stability in terms of resting membrane potential, input resistance, holding duration and spike magnitude, to manual *in vivo* studies (Margrie et al., 2002; DeWeese, 2007) and "blind" robotic systems (Kodandaramaiah et al., 2012, 2018), across a range of recording depths. For more information on the state-of-the-art in autonomous patch-clamping, consult the reviews by Annecchino and Schultz (2018), Suk et al. (2019) and Alegria et al. (2020).

6 Overview

Patch-clamp is among the most effective tools for obtaining high-fidelity electrical recordings of individual neurons and has enabled the analysis of cell excitability, post and presynaptic responses, neuronal inter-connectivity and high order behavioural states, among many others. Despite providing high-quality data, the patch-clamp technique remains limited by the inherent low throughput and labour intensity. For an experienced experimenter, success rates for "blind" whole-cell *in vivo* recordings are reported to fall between 20 - 50% (Margrie et al., 2002). Robotic automation helps mitigating such issues and offers several benefits including faster skill assimilation for operators new to the technique, standardised recording quality, and improved throughput. It also opens up the potential to reliably scaling up the technique to simultaneous patch-clamp recording from multiple cells *in vivo*, enabling assays of synaptic coupling and many new research lines in basic and translational neuroscience. Significant strides have been made towards the automation of both "blind" and two-photon guided approaches as evidenced by the numerous systems presented. Automated blind systems can achieve success rates comparable to human experimenters with improved throughput, and have expanded to patch up to three cells simultaneously. Targeted multi-patching, however, is yet to be realised due to the difficulties associated with controlling multiple pipettes simultaneously and constraints of two-photon imaging. Automated patch-clamp systems can be further improved and optimised to realise the full capabilities of the technique.

Bibliography

Alegria, A., Joshi, A., O'Brien, J., and Kodandaramaiah, S. B. (2020). Single neuron recording: progress towards high-throughput analysis.

Andrásfalvy, B. K., Galiñanes, G. L., Huber, D., Barbic, M., Macklin, J. J., Susumu, K., Delehanty, J. B., Huston, A. L., Makara, J. K., and Medintz, I. L. (2014). Quantum dot-based multiphoton fluorescent pipettes for targeted neuronal electrophysiology. *Nature Methods*, 11(12):1237–1241.

Annecchino, L. (2016). *Development and validation of a robotic two-photon targeted whole-cell recording system for in vivo electrophysiology*. PhD thesis, Imperial College London.

Annecchino, L. A., Morris, A. R., Copeland, C. S., Agabi, O. E., Chadderton, P., and Schultz, S. R. (2017). Robotic automation of in vivo two-photon targeted whole-cell patch-clamp electrophysiology. *Neuron*, 95(5):1048–1055.

Annecchino, L. A. and Schultz, S. R. (2018). Progress in automating patch clamp cellular physiology. *Brain and Neuroscience Advances*, 2:2398212818776561.

Cadwell, C. R., Palasantza, A., Jiang, X., Berens, P., Deng, Q., Yilmaz, M., Reimer, J., Shen, S., Bethge, M., Tolias, K. F., et al. (2016). Electrophysiological, transcriptomic and morphologic profiling of single neurons using patch-seq. *Nature Biotechnology*, 34(2):199–203.

Crochet, S. and Petersen, C. C. (2006). Correlating whisker behavior with membrane potential in barrel cortex of awake mice. *Nature Neuroscience*, 9(5):608–610.

Desai, N. S., Siegel, J. J., Taylor, W., Chitwood, R. A., and Johnston, D. (2015). Matlab-based automated patch-clamp system for awake behaving mice. *Journal of Neurophysiology*, 114(2):1331–1345.

DeWeese, M. R. (2007). Whole-cell recording in vivo. *Current Protocols in Neuroscience*, 38(1):6–22.

Ghanbari, L., Rynes, M. L., Hu, J., Schulman, D. S., Johnson, G. W., Laroque, M., Shull, G. M., and Kodandaramaiah, S. B. (2019). Craniobot: A computer numerical controlled robot for cranial microsurgeries. *Scientific Reports*, 9(1):1–12.

Hamill, O. P., Marty, A., Neher, E., Sakmann, B., and Sigworth, F. (1981). Improved patch-clamp techniques for high-resolution current recording from cells and cell-free membrane patches. *Pflügers Archiv*, 391(2):85–100.

Holst, G. L., Stoy, W., Yang, B., Kolb, I., Kodandaramaiah, S. B., Li, L., Knoblich, U., Zeng, H., Haider, B., Boyden, E. S., et al. (2019). Autonomous patch-clamp robot for functional characterization of neurons in vivo: development and application to mouse visual cortex. *Journal of Neurophysiology*, 121(6):2341–2357.

Jouhanneau, J.-S. and Poulet, J. F. (2019). Multiple two-photon targeted whole-cell patch-clamp recordings from monosynaptically connected neurons in vivo. *Frontiers in Synaptic Neuroscience*, 11:15.

Kitamura, K., Judkewitz, B., Kano, M., Denk, W., and Häusser, M. (2008). Targeted patch-clamp recordings and single-cell electroporation of unlabeled neurons in vivo. *Nature Methods*, 5(1):61–67.

Kodandaramaiah, S. B., Flores, F. J., Holst, G. L., Singer, A. C., Han, X., Brown, E. N., Boyden, E. S., and Forest, C. R. (2018). Multi-neuron intracellular recording in vivo via interacting autopatching robots. *Elife*, 7:e24656.

Kodandaramaiah, S. B., Franzesi, G. T., Chow, B. Y., Boyden, E. S., and Forest, C. R. (2012). Automated whole-cell patch-clamp electrophysiology of neurons in vivo. *Nature Methods*, 9(6):585–587.

Kodandaramaiah, S. B., Holst, G. L., Wickersham, I. R., Singer, A. C., Franzesi, G. T., McKinnon, M. L., Forest, C. R., and Boyden, E. S. (2016). Assembly and operation of the autopatcher for automated intracellular neural recording in vivo. *Nature Protocols*, 11(4):634.

Kolb, I., Landry, C. R., Yip, M. C., Lewallen, C. F., Stoy, W. A., Lee, J., Felouzis, A., Yang, B., Boyden, E. S., Rozell, C. J., et al. (2019). Patcherbot: a single-cell electrophysiology robot for adherent cells and brain slices. *Journal of Neural Engineering*, 16(4):046003.

Kolb, I., Stoy, W., Rousseau, E., Moody, O., Jenkins, A., and Forest, C. (2016). Cleaning patch-clamp pipettes for immediate reuse. *Scientific Reports*, 6(1):1–10.

Koos, K., Oláh, G., Balassa, T., Mihut, N., Rózsa, M., Ozsvár, A., Tasnadi, E., Barzó, P., Faragó, N., Puskás, L., et al. (2021). Automatic deep learning-driven label-free image-guided patch clamp system. *Nature Communications*, 12(1):1–11.

Landry, C. R., Yip, M. C., Kolb, I., Stoy, W. A., Gonzalez, M. M., and Forest, C. R. (2021). Method for rapid enzymatic cleaning for reuse of patch clamp pipettes: Increasing throughput by eliminating manual pipette replacement between patch clamp attempts. *Bio-Protocol*, 11(14):4085.

Lin, M. Z. and Schnitzer, M. J. (2016). Genetically encoded indicators of neuronal activity. *Nature Neuroscience*, 19(9):1142.

Long, B., Li, L., Knoblich, U., Zeng, H., and Peng, H. (2015). 3d image-guided automatic pipette positioning for single cell experiments in vivo. *Scientific Reports*, 5(1):1–8.

Margrie, T. W., Brecht, M., and Sakmann, B. (2002). In vivo, low-resistance, whole-cell recordings from neurons in the anaesthetized and awake mammalian brain. *Pflügers Archiv*, 444(4):491–498.

Markram, H., Lübke, J., Frotscher, M., and Sakmann, B. (1997). Regulation of synaptic efficacy by coincidence of postsynaptic aps and epsps. *Science*, 275(5297):213–215.

Mun, J., Camarena, A., Walker, C., Lin, M. Y., Wolseley, V., Souaiaia, T., Thornton, M., Grubbs, B., Chow, R. H., Evgrafov, O. V., et al. (2020). Robust rna-seq of arna-amplified single cell material collected by patch clamp. *Scientific Reports*, 10(1):1–9.

Otsu, N. (1979). A threshold selection method from gray-level histograms. *IEEE Transactions on Systems, Man, and Cybernetics*, 9(1):62–66.

Pei, X., Vidyasagar, T., Volgushev, M., and Creutzfeldt, O. (1994). Receptive field analysis and orientation selectivity of postsynaptic potentials of simple cells in cat visual cortex. *Journal of Neuroscience*, 14(11):7130–7140.

Peng, Y., Mittermaier, F. X., Planert, H., Schneider, U. C., Alle, H., and Geiger, J. R. P. (2019). High-throughput microcircuit analysis of individual human brains through next-generation multineuron patch-clamp. *Elife*, 8:e48178.

Perin, R. and Markram, H. (2013). A computer-assisted multi-electrode patch-clamp system. *Journal of Visualized Experiments: JoVE*, e50630(80).

Rynes, M. L., Ghanbari, L., Schulman, D. S., Linn, S., Laroque, M., Dominguez, J., Navabi, Z. S., Sherman, P., and Kodandaramaiah, S. B. (2020). Assembly and operation of an open-source, computer numerical controlled (cnc) robot for performing cranial microsurgical procedures. *Nature Protocols*, 15(6):1992–2023.

Stoy, W. A., Kolb, I., Holst, G., Liew, Y., Pala, A., Yang, B., Boyden, E. S., Stanley, G. B., and Forest, C. R. (2017). Robotic navigation to subcortical neural tissue for intracellular electrophysiology in vivo. *Journal of Neurophysiology*, 118(2):1141–1150.

Stoy, W. M., Yang, B., Kight, A., Wright, N. C., Borden, P. Y., Stanley, G. B., and Forest, C. R. (2021). Compensation of physiological motion enables high-yield whole-cell recording in vivo. *Journal of Neuroscience Methods*, 348:109008.

Suk, H.-J., Boyden, E. S., and van Welie, I. (2019). Advances in the automation of whole-cell patch clamp technology. *Journal of Neuroscience Methods*, 326:108357.

Suk, H.-J., van Welie, I., Kodandaramaiah, S. B., Allen, B., Forest, C. R., and Boyden, E. S. (2017). Closed-loop real-time imaging enables fully automated cell-targeted patch-clamp neural recording in vivo. *Neuron*, 95(5):1037–1047.

Wu, Q. and Chubykin, A. A. (2017). Application of automated image-guided patch clamp for the study of neurons in brain slices. *Journal of Visualized Experiments: JoVE*, 56010(125).

Wu, Q., Kolb, I., Callahan, B. M., Su, Z., Stoy, W., Kodandaramaiah, S. B., Neve, R., Zeng, H., Boyden, E. S., Forest, C. R., et al. (2016). Integration of autopatching with automated pipette and cell detection in vitro. *Journal of Neurophysiology*, 116(4):1564–1578.

Yang, H. H. and St-Pierre, F. (2016). Genetically encoded voltage indicators: opportunities and challenges. *Journal of Neuroscience*, 36(39):9977–9989.